Nonclassical Field Dynamics in Photonic Band Structures: Atomic-Beam Resonant Interaction with a Spatially Periodic Field Mode

B. Sherman, G. Kurizki, and A. Kadyshevitch

Department of Chemical Physics, Weizmann Institute of Science, Rehovot 76100, Israel

(Received 1 June 1992)

We consider the quantum electrodynamics of an atom uniformly moving through a single spatially periodic field mode. The shape and periodicity of the field modulation can be designed by an appropriate choice of a defect in a periodic structure that possesses a forbidden spectral band (a "photonic band gap"). The design of the periodic modulation can improve our control over the evolution and properties (e.g., photon statistics) of nonclassical "Schrödinger-cat" states of the field, generated by resonant interaction with the atom.

PACS numbers: 42.50.Dv, 42.25.−p, 42.50.Md, 78.65.−s

The quest for quantum electrodynamical (QED) effects in atomic interactions with electromagnetic fields has achieved spectacular success in studies of atomic-beam propagation through high-Q single-mode microcavities. The focus of these studies are dynamical effects conforming to the Jaynes-Cummings model (JCM), which describes the interaction of a two-level atom with a single field mode that is *spatially uniform* along the atomic path [1–3]. An intriguing feature of the JCM dynamics is that a field initially prepared in a quasiclassical coherent state can evolve into a "Schrödinger cat": a superposition of two quasiclassical states with different mean amplitudes or phases [4,5]. The initial quasiprobability distribution (Q function) of the field is split by the interaction (via a purely unitary evolution [6,7], or via atomic-state preselection or postselection [8–10]) into two parts that counterrotate in the phase plane, alternating between a "cat" state as they move far apart, and approximate restoration of the initial field state as they overlap [5–7]. Nonclassical properties of the field, such as sub-Poissonian or oscillatory photon statistics and quadrature squeezing, arise during the partial overlap of the two Q-function parts [4,11]. The alternate splitting and restoration of the Q function correspond to the dephasing ("collapse") and rephasing ("revival") of the oscillating terms in the atomic population inversion, each term having a Rabi frequency associated with a different photon number that contributes to the field [5,6].

These features of the JCM dynamics are currently viewed as fundamental manifestations of the QED nature of the field. Yet we may ask how sensitive the JCM dynamics is to the assumption, which is justified in existing experimental setups [3,9], that the field is effectively uniform along the atomic path. We shall consider here an atomic beam propagating along and interacting with a spatially periodic field mode on resonance. For atoms that are sufficiently fast (with velocities above 10^4 cm/sec) and low photon numbers, there is practically no spatial diffraction or velocity change due to the field [12], whence such spatial modulation is equivalent to periodic temporal modulation of the field-atom coupling. In its simplest form, this modulation is sinusoidal, as in the case of a high-order mode of a micromaser cavity. It is particularly timely to examine this situation with the advent of novel structures, wherein all field modes can be inhibited by the periodicity of the dielectric index in a spectral band of forbidden dispersion, known as a photonic band gap [13,14]. An allowed mode may be formed at a chosen frequency within the band gap near a defect that disrupts the structure periodicity [15]. An atomic beam propagating through a void in such a defect can resonantly interact with this mode (Fig. 1). The appeal of such a defect mode is that it can be designed to exhibit *any desired* periodic or aperiodic modulation, not merely sinusoidal. Its realization appears to be presently feasible in the microwave domain (provided that low-absorption materials are used, so as to achieve high-Q values) [13,15]. In the near future a single-mode field-atom interaction (with negligible coupling to the continuum) at an *optical* frequency promises to be more realizable in such a structure than in a cavity [16].

As shown here, periodic temporal modulation of the resonant field-atom coupling can drastically modify the prominent dynamical features of the JCM, such as the evolution of Schrödinger cats and the corresponding oscillations of the atomic population inversion [17]. In addition to their inherent novelty and interest, these modified features are shown to allow better control than their JCM counterparts over the generation and properties of nonclassical field states. In particular, the photon statistics is shown to be governed by both the periodicity and the *modulation shape* of the field mode, thus demonstrating the advantages of an appropriately designed defect.

The resonant interaction of a two-level atom moving at a constant velocity $\mathbf{v}_z$ through a spatially modulated single-mode field is described by the Hamiltonian [2]

$$H_I=\hbar\Omega(\mathbf{r}(t))(\sigma_+a+\sigma_-a^\dagger). \tag{1}$$

Here σ_+ (σ_-) and $a^\dagger$ (a) are the dipole and field raising (lowering) operators, respectively, whereas

$$\hbar\Omega(\mathbf{r}(t))=(\hbar\omega/2)^{1/2}(\mu_{eg}\cdot\hat{\epsilon}_\lambda)g_\lambda(\mathbf{r}=\mathbf{v}_zt+\mathbf{r}_\perp) \tag{2}$$

is the coupling energy of the vacuum field to the dipole moment μ_{eg} for the atomic transition $e\rightarrow g$, normalized in the structure volume V and having the resonant frequency $\omega=\omega_{eg}$. The polarization vector of the field mode

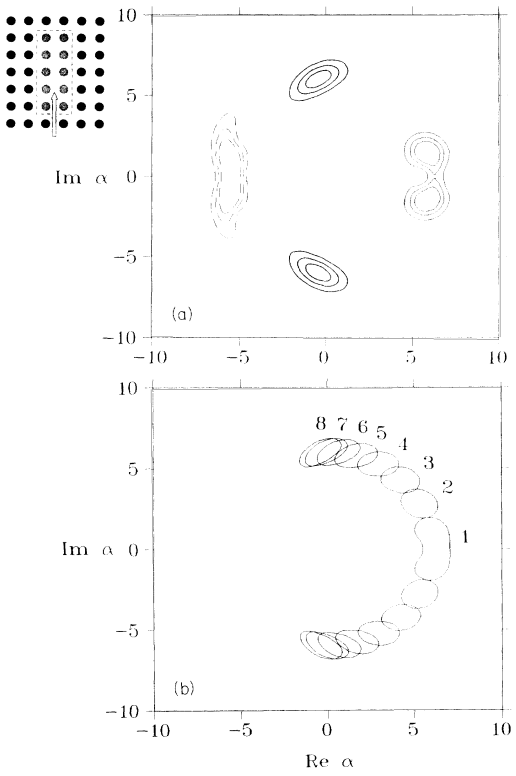

FIG. 1. Inset: Atomic-beam propagation through a rectangular defect in a square lattice of dielectric rods. (a) Q function of conditionally prepared Schrödinger cats evolving from a coherent state ($\alpha_0=6$) for an atom moving in resonant periodic mode. The cats are drawn in the phase plane at $\phi_{\max}=\chi/\alpha_0$ for different χ: thin contour, $\phi_{\max}=0.5$; thick contours, $\phi_{\max}\approx\pi$; dashed contour, $\phi_{\max}\approx 2\pi$. (b) Snapshots of the T evolution of the thick-contour Q function at intervals of $\omega_D\Delta T=0.2$. Note the sluggishness (freezing) near $\phi_{\max}\approx\pi$.

is $\hat{\boldsymbol{\epsilon}}_\lambda$ and its spatial amplitude $g_\lambda(\mathbf{r})$ is the eigenfunction of the wave equation in the structure for either E or H polarization.

In this Letter we shall consider structures in which (see below) the single-mode eigenfunction $g_\lambda(\mathbf{r})$ is a real, periodic function of $z=v_z t$ (a standing wave in z). The advantage of a real $g_\lambda(\mathbf{r}(t))$ is that it allows the straightforward derivation of the evolution operator $U(t)$ for the entangled field-atom system governed by Eq. (1). In analogy with Ref. [18] (in which Ω is time independent), we can show that

$$U(t)=\tfrac{1}{2}(1+\sigma_3)\cos\gamma(t)+\tfrac{1}{2}(1-\sigma_3)\cos\beta(t) -i\sigma_+ a\beta^{-1}(t)\sin\beta(t)-i\sigma_- a^\dagger\gamma^{-1}(t)\sin\gamma(t)\,. \tag{3}$$

Here σ_3 is the operator of atomic inversion, and

$$\beta(t)=(a^\dagger a)^{1/2}\theta(t),\quad \gamma(t)=(aa^\dagger)^{1/2}\theta(t)\,, \quad \theta(t)=\int_0^t\Omega(t')dt'\,. \tag{4}$$

As implied by Eqs. (3) and (4), the evolution of all atomic and field observables is governed by the initial field distribution (or photon statistics), and the adiabatic phase $\theta(t)$, which is proportional to the integral of $g_\lambda(\mathbf{r}(t))$ over the atomic interaction (passage) time. We therefore proceed to specify the field eigenfunctions $g_\lambda(\mathbf{r}(t))$.

In addition to Fabry-Pérot or micromaser cavity eigenfunctions, we consider here the mode eigenfunctions of a nearly periodic square lattice of rods with dielectric index ϵ_1 that are aligned in the y direction, so that the dielectric index ϵ of the structure varies with x and z. By applying a magnetic field to the atoms, the dipole moment μ_{eg} is selected to interact only with a y-polarized electromagnetic field, whose mode eigenfunction satisfies the two-dimensional (2D) *scalar* wave equation [19]

$$[(d^2/dx^2+d^2/dz^2)+\epsilon(x,z)\omega^2/c^2]g_y=0\,. \tag{5}$$

A perfectly periodic square lattice with period P can display appreciable photonic band gaps for the y polarization [19], even for moderate modulations of $\epsilon(x,z)$ between ϵ_1 and 1. On replacing, say, two z-directed rows of rods over a distance $L_z\gg P$ by rods with $\epsilon_2\neq\epsilon_1$, a rectangular defect is created, with $L_z\gg L_x=2P$ [Fig. 1(a)]. The eigenfunctions of local modes formed by such a defect at discrete ω within the band gaps can be approximated, in *complete analogy* to electronic eigenfunctions of semiconductor heterostructures with similar geometries [20], to have the factorized form $g_y(\omega,\mathbf{r})\approx\varphi_y(x,z)F_1(\omega,x)F_2(\omega,z)$. Here $\varphi_y(x,z)$ is a periodic, standing-wave eigenfunction of the perfect square lattice, evaluated at the allowed-band extremum nearest to ω. For $\epsilon_2<\epsilon_1$, discrete "acceptor" modes [15] will arise just above the top of the lowest E polarization band, which corresponds to a frequency ω_0 and wave vector $\mathbf{k}_0=-(\pi/P)(\hat{\mathbf{x}}+\hat{\mathbf{z}})$ [19]. Then, $\varphi_y(x,z)$ can be written in the z-periodic form

$$\varphi_y(x,z)=\sum_j c_j(x)\cos(j\pi z/P) \tag{6}$$

whose Fourier coefficients $c_j(x)$ are obtainable either numerically [19] or analytically (in exceptional cases [21]). The factors F_1 and F_2 are envelope functions, each solving a 1D wave equation with the *averaged* "square-well potential" [20] $[\omega_0^2(\epsilon_2-\epsilon_1)/c^2]$ (for x or z within the defect). The envelopes F_1 or F_2 therefore oscillate within the defect, exponentially decaying outside of it (for the lowest-order mode, $F_1F_2\sim\cos K_x x\cos K_z z$, with $K_{x(z)}\sim\pi/L_{x(z)}$). Then, for an atomic beam collimated to pass well within the defect, we obtain from Eqs. (4) and (6)

$$\theta(T=L_z/v_z)\approx(\chi/2)\sum_j[c_j(x=0)/j][\sin(j\omega_D T+\delta)+\sin(j\omega_D T-\delta)] \tag{7}$$

Here [Eqs. (1) and (2)]

$$\chi=(\omega/2\hbar)^{1/2}(\mu_{eg})F_1(\omega,x=0)/\omega_D \tag{8}$$

is the ratio of the vacuum Rabi frequency (for a static atom) to $\omega_D = \pi v_z/P$, which is the Doppler shift at the resonant wave vector, or, equivalently, the inverse time to traverse $P/2$. The envelope-function phase $\delta \sim \omega_D T(P/L_z)$ will be *neglected* in what follows. For a Fabry-Pérot or micromaser cavity eigenfunction, Eq. (7) is purely sinusoidal, i.e., it has the $j=1$ term only. As shown below, it may be advantageous to use structures in which the field and atom evolve with *multiple harmonics* of ω_D, whose weight c_j/j is appreciable.

The first feature to be evaluated here by means of Eqs. (3), (4), and (7) is the evolution of the mean atomic inversion $\langle \sigma_z(T) \rangle$ for an initially excited atom and a field initially specified in the number-state representation by the density operator $\rho_F(0) = \sum_{nn'} \rho_{nn'}(0) |n\rangle\langle n'|$. We find

$$\langle \sigma_3(T) \rangle = \mathrm{Tr}[\rho_F(0) U(T) \sigma_3(0) U^\dagger(T)] = \sum_{n=0,1,\ldots} \rho_{nn}(0) \cos[2(n+1)^{1/2}\theta(T)]$$

$$= \sum_n \rho_{nn}(0) \prod_{j=1}^{\infty} [J_0(A_{n,j}) + \sum_p J_{2p}(A_{n,j}) \cos(2jp\omega_D T)] , \tag{9}$$

where $A_{n,j} = 2(n+1)^{1/2}\chi c_j/j$. The last equality in Eq. (9) follows from the expansion of a cosine of an odd periodic argument in terms of Bessel functions. The periodicity of $\theta(T)$ compels $\langle \sigma_z(T) \rangle$ to exhibit a periodic pattern of collapses and revivals, *regardless of the initial photon statistics*. Thus, revivals occur when $\theta(T) = 0$, corresponding to $\omega_D T = 0, \pi, 2\pi, \ldots$. This property of the inversion is in sharp contrast to its counterpart in the ordinary JCM, wherein only Poissonian or sub-Poissonian photon statistics can yield distinct revivals [1,2]. However, the initial photon statistics $\rho_{nn}(0)$ still plays an important role in the temporal patterns of Eq. (9), in that it determines, along with $\chi c_j/j$, the number of contributing (interfering) harmonics $jp\omega_D$, and thereby the width of the dephasing intervals. The broad photon-number distribution of the thermal field causes the higher harmonics to coalesce, forming broad dephasing intervals. Narrower dephasing intervals (or wider oscillation revivals) obtain for the Poissonian photon-number distribution (a coherent field) with the same $\langle n \rangle$ and χc_j, since fewer $A_{n,j}$ contribute. For an initial vacuum state, only $\chi c_j/j$ determines the number of harmonics and the modulation depth [17]. In the limit $A_{n,j} \ll 1$ (corresponding to low $\langle n \rangle$ and/or an atom traversing $P/2$ much *faster* than a vacuum Rabi cycle), the leading term of $J_{2p}(A_{n,j})$ implies that only the harmonics with $p=1$ and j such that $c_j/j \sim c_1$ are appreciable in Eq. (9). Thus, the atomic evolution is also controllable by the form of spatial modulation, which determines the c_j in Eq. (7).

The collapses and revivals of the atomic inversion are paralleled by the splitting (dephasing) and restoration (rephasing) of the quasiprobability distribution that characterizes the field. In what follows, the initial conditions are assumed to be an atom in the excited state $|e\rangle$ and a coherent field state $|\alpha_0\rangle$, with $|\alpha_0| \gg 1$. As the atoms emerge from the structure at time T, the ensemble of excited atoms is selected. This conditional measurement [10] projects out the following field density operator, using Eqs. (3) and (4):

$$\rho_F^{(e)}(T) = C[\langle e|U(T)\rho_F(0)(|e\rangle\langle e|)U^\dagger(T)|e\rangle] = \sum_{nn'} \rho_{nn'}(0) \cos[(n+1)^{1/2}\theta(T)] \cos[(n'+1)^{1/2}\theta(T)] (|n\rangle\langle n'|) , \tag{10}$$

where C is a normalizing constant. The Q function associated with Eq. (10), i.e., the diagonal element of $\rho_F^{(e)}$ with respect to a coherent state $|\alpha\rangle$, is found to be, for the chosen initial conditions, to first order in the deviation $n - \langle n \rangle = n - |\alpha_0|^{1/2}$,

$$Q_\alpha(T) = \langle \alpha|\rho_F^{(e)}|\alpha\rangle \approx (C/4)\exp(-|\alpha|^2 - |\alpha_0|^2) \left| \exp[i|\alpha|\theta(T)/2] \sum_n \{\alpha^* \alpha_0 \exp[i\theta(T)/2|\alpha_0|]\}^n/n! + (\theta \to -\theta) \right| . \tag{11}$$

This form implies that $Q_\alpha(T)$ has two peaks, at $\alpha_{1,2} = \alpha_0 \exp[\pm i\theta(T)/2|\alpha_0|]$, corresponding to two superposed parts of the Q function. Hence, the field evolves into a Schrödinger cat superposition when the mean relative phase $\phi = \theta(T)/|\alpha_0|$ is large enough to make the two Q-function parts nonoverlapping.

Two properties distinguish the cat behavior of Eq. (11) from its JCM counterpart [4–7]: (a) The cat is constrained to oscillate periodically in $\omega_D T$ between $\phi_{\min} = 0$ and [Eq. (7)] $\phi_{\max} = \chi \sum_j (c_j/j) \sin(j\pi/2)/|\alpha_0|$ [Fig. 1(a)]. Collapses and revivals of the atomic inversion occur, respectively, as ϕ alternates between large values, corresponding to nonoverlapping parts of the Q function, and small values, for which the initial Q function is roughly restored. In the limit $\chi \leq 1$, $\phi_{\max}$ is so small that the Q function remains strongly overlapping at any T (no collapses). By contrast, in the ordinary JCM the relative phase between the split Q-function parts is unconstrained in T, going through successive periods of 2π. (b) Near the maximum relative phase $\phi_{\max}$ the cat evolution is sluggish, as the counterrotation rate of the two Q-function parts is then $\dot{\phi} \approx \dot{\theta}/|\alpha_0| \approx 0$ [Eq. (7)]. Hence, the cat is nearly "frozen" near $\phi_{\max}$ [Fig. 1(b)], whereas its JCM counterpart evolves at a roughly constant rate of $\dot{\phi} \approx \Omega/\alpha_0$ [Ω being the vacuum Rabi frequency as in Eq. (2), but without temporal modulation].

Nonclassical (sub-Poissonian or oscillatory) photon statistics and quadrature squeezing are obtained whenever the two parts of the Q function partly overlap [4]. The advantage of the field evolution considered here is that the T interval over which the required overlap persists is controlled by χ and $|\alpha_0|$. Consequently, one can achieve sub-Poisson statistics for a considerably wider and more

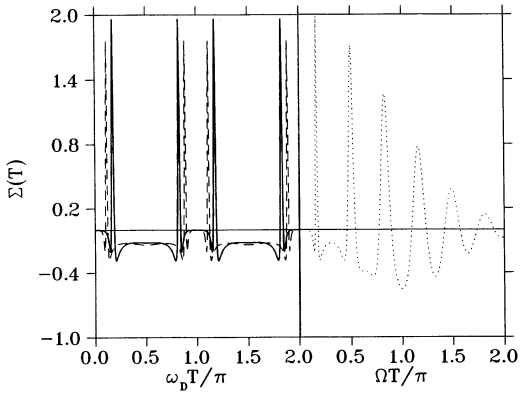

FIG. 2. Left: Photon statistics of an overlapping Q function ($\chi=0.5$, $\alpha_0=6$), evolving similarly to thin contour in Fig. 1. The Mandel parameter $\Sigma=(\langle\Delta n^2\rangle-\langle n\rangle)/\langle n\rangle$, where $\langle\Delta n^2\rangle$ is the photon-number variance, is plotted vs $\omega_D T/\pi$. $\Sigma<0$ corresponds to sub-Poissonian statistics. Solid curve, sinusoidal modulation; dashed curve, periodic modulation with significant third harmonic ($c_3/c_1=0.6$), resulting in wider sub-Poissonian intervals. Right: *idem*, for ordinary JCM (dotted curve).

regular range of T intervals than in the ordinary JCM (Fig. 2). We have verified numerically that the sub-Poissonian features of our model are less sensitive to a Gaussian spread in velocities, or in α_0, than their JCM counterparts.

The spatial modulation shape can also help control the field evolution and its photon statistics. Higher harmonics (c_j with $j>1$) introduce additional minima or maxima into the T dependence of θ [Eq. (7)]. Hence, there are more points near which the rate ϕ vanishes, and the Q function is frozen. The resulting effect on photon statistics is demonstrated in Fig. 2.

To conclude, the interplay between the initial quantum distribution and the spatial periodicity of a single-mode field at resonance with a uniformly moving atom has been shown to yield unique, intriguing dynamical features: (i) The atomic population inversion exhibits periodic oscillation "revivals," for *any* initial field state, even a classical-like thermal distribution. (ii) Superposed quasiclassical field states (Schrödinger cats) periodically alternate between complete overlap and a maximal phase separation $\phi_{\max}$, which is *adjustable* by the atomic velocity and/or mean photon number, as opposed to the unrestricted variation of the phase separation in cats governed by the JCM [5,6]. (iii) By selecting the velocity and spatial modulation shape, the cat can be nearly frozen for the desired fraction of the evolution period near the extremum points of its phase separation, a feature that has no analog in ordinary JCM cats. When this freezing corresponds to an overlap of the two cat parts, sub-Poissonian photon statistics results for a much wider range of interaction times than in the JCM. Consequently, the present model can achieve enhanced stability of nonclassical field properties against fluctuations of the atomic velocity or the initial field preparation (e.g., initial statistical spread of coherent states).

This work has been supported by the U.S.-Israel Binational Science Foundation. B.S. is supported by a grant from the Bat-Sheva Foundation.

[1] J. H. Eberly, N. B. Narozhny, and J. J. Sanchez-Mondragon, Phys. Rev. Lett. **44**, 1323 (1980).
[2] P. L. Knight and P. M. Radmore, Phys. Rev. A **26**, 676 (1982).
[3] G. Rempe, H. Walther, and N. Klein, Phys. Rev. Lett. **58**, 353 (1987); G. Rempe, F. Schmidt-Kaler, and H. Walther, Phys. Rev. Lett. **64**, 2783 (1990).
[4] W. Schleich, M. Pernigo, and Fam Le Kien, Phys. Rev. A **44**, 2172 (1991).
[5] J. Eiselt and H. Risken, Opt. Commun. **72**, 351 (1989).
[6] J. Gea-Banacloche, Phys. Rev. Lett. **65**, 3385 (1990); Phys. Rev. A **44**, 5913 (1991).
[7] S. J. D. Phoenix and P. L. Knight, Ann. Phys. (N.Y.) **186**, 381 1988); Phys. Rev. Lett. **66**, 2833 (1991); Phys. Rev. A **44**, 6023 (1991); J. Opt Soc. Am. B **7**, 116 (1990).
[8] P. Meystre, J. J. Slosser, and M. Wilkens. Opt. Commun. **79**, 300 (1990); C. M. Savage, S. L. Braunstein, and D. F. Walls, Opt. Lett. **15**, 628 (1990).
[9] M. Brune, S. Haroche, J. M. Raimond, L. Davidovich, and N. Zagury, Phys. Rev. A **45**, 5193 (1992).
[10] B. Sherman and G. Kurizki, Phys. Rev. A **45**, 7674 (1992).
[11] V. Bužek and P. L. Knight, Opt. Commun. **81**, 331 (1991).
[12] S. Haroche, M. Brune, and J. M. Raimond, Europhys. Lett. **14**, 19 (1991); A. P. Kazantsev, G. J. Surdutovich, and V. P. Yakovlev, *Mechanical Action of Light* (World Scientific, Singapore, 1990).
[13] E. Yablonovitch, Phys. Rev. Lett. **58**, 2059 (1987); E. Yablonovitch, T. J. Gmitter, and K. M. Leung, Phys. Rev. Lett. **67**, 2295 (1991).
[14] K. M. Leung and Y. F. Liu, Phys. Rev. Lett. **65**, 2646 (1990); K. M. Ho, C. T. Chan, and C.M. Soukolis, Phys. Rev. Lett. **65**, 3150 (1990).
[15] E. Yablonovitch, T. J. Gmitter, R. D. Meade, A. M. Rappe, K. D. Brommer, and J. D. Joannopoulos, Phys. Rev. Lett. **67**, 3380 (1991).
[16] S. E. Morin, Q. Wu, and T. W. Mossberg, Opt. Phot. News **3**, 3 (1992).
[17] Sinusoidal oscillations of the population inversion in the case of initial vacuum field have been recently analyzed for an atomic beam along a Fabry-Pérot cavity axis, by G. M. Palma and F. S. Persico, Europhys. Lett. **17**, 207 (1992) and P. Meystre, Opt. Commun. (to be published).
[18] S. Singh, Phys. Rev. A **25**, 3206 (1982).
[19] M. Plihal, A. Shambrook, and A. A. Maradudin, Opt. Commun. **80**, 199 (1991).
[20] See the effective-mass approximation (EMA) treatment of a 2D "quantum wire," e.g., Y. Arakawa and A. Yariv, IEEE J. Quantum Electron. **22**, 1887 (1986). For an EMA treatment of other ("shallow") defects, see S. Pantelides, Rev. Mod. Phys. **50**, 797 (1978).
[21] If $\epsilon(x,z)$ is a sum of 1D periodic $\epsilon(x)$ and $\epsilon(z)$, then the eigenfunctions can be analytically approximated by treatment of the 1D Hill equation, e.g., G. Kurizki, Phys. Rev. B **33**, 49 (1986).

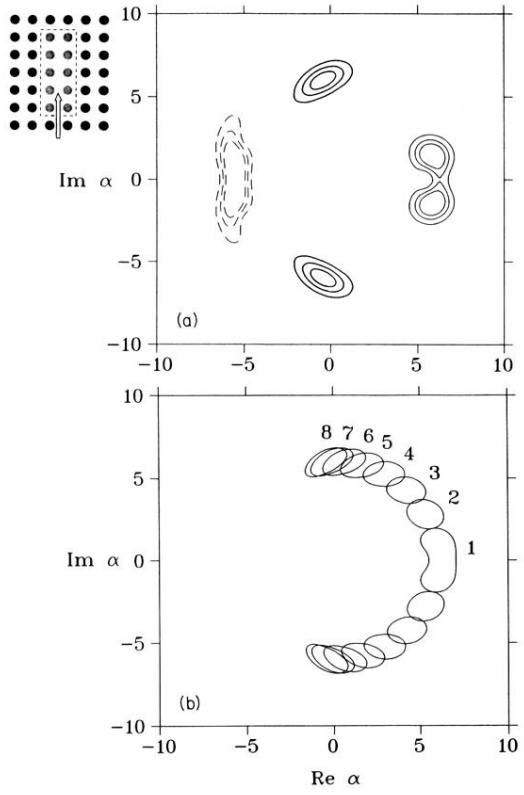

FIG. 1. Inset: Atomic-beam propagation through a rectangular defect in a square lattice of dielectric rods. (a) Q function of conditionally prepared Schrödinger cats evolving from a coherent state ($\alpha_0=6$) for an atom moving in resonant periodic mode. The cats are drawn in the phase plane at $\phi_{\max}=\chi/\alpha_0$ for different χ: thin contour, $\phi_{\max}=0.5$; thick contours, $\phi_{\max}\approx\pi$; dashed contour, $\phi_{\max}\approx 2\pi$. (b) Snapshots of the T evolution of the thick-contour Q function at intervals of $\omega_D\Delta T=0.2$. Note the sluggishness (freezing) near $\phi_{\max}\approx\pi$.